



## Mechanical and environmental performance of cementitious materials containing activated carbon contaminated with trivalent chromium

Amina Azarrih, Lyacine Bennacer, Kheira Bouragaa, Benammar Balegh

Online Publication Date: 20 September 2025

URL: <http://www.jresm.org/archive/resm2025-977me0618rs.html>

DOI: <http://dx.doi.org/10.17515/resm2025-977me0618rs>

Journal Abbreviation: *Res. Eng. Struct. Mater.*

### To cite this article

Azarrih A, Bennacer L, Bouragaa K, Balegh B. Mechanical and environmental performance of cementitious materials containing activated carbon contaminated with trivalent chromium. *Res. Eng. Struct. Mater.*, 2026; 12(3): 1487-1499.

### Disclaimer

All the opinions and statements expressed in the papers are on the responsibility of author(s) and are not to be regarded as those of the journal of Research on Engineering Structures and Materials (RESM) organization or related parties. The publishers make no warranty, explicit or implied, or make any representation with respect to the contents of any article will be complete or accurate or up to date. The accuracy of any instructions, equations, or other information should be independently verified. The publisher and related parties shall not be liable for any loss, actions, claims, proceedings, demand or costs or damages whatsoever or howsoever caused arising directly or indirectly in connection with use of the information given in the journal or related means.



Published articles are freely available to users under the terms of Creative Commons Attribution - NonCommercial 4.0 International Public License, as currently displayed at [here](#) (the "CC BY - NC").

Research Article

## Mechanical and environmental performance of cementitious materials containing activated carbon contaminated with trivalent chromium

Amina Azarrih <sup>\*1,a</sup>, Lyacine Bennacer <sup>2,3,b</sup>, Kheira Bouragaa <sup>1,c</sup>, Benammar Balegh <sup>4,d</sup>

<sup>1</sup>Department of Civil Engineering, University of Adrar, Laboratory of Sustainable Development and IT, LDDI, Adrar, Algeria

<sup>2</sup>Department of Civil Engineering, University of Adrar, Laboratory of Energy, Environment and Information System, LEESI, Adrar, Algeria

<sup>3</sup>Department of Civil Engineering, University of Adrar, LGCE Laboratory, Adrar, Algeria

<sup>4</sup>Department of Civil Engineering, University of Adrar, Laboratory of Civil and Environmental Engineering in Saharan Regions, LGCEMS, Adrar, Algeria

### Article Info

### Abstract

#### Article History:

Received 18 June 2025

Accepted 19 Sep 2025

#### Keywords:

Cement;  
Trivalent chromium;  
Activated biochar;  
Mechanical strength;  
Incorporation

Trivalent chromium (Cr(III)) from the tanning industry presents considerable environmental hazards due to its bio accumulative toxicity. This work investigates a sustainable waste management approach by incorporating Cr(III)-contaminated activated carbon (AC) into cementitious materials. The primary aim was to assess the mechanical properties of cement mortars, including different concentrations of contaminated AC—specifically, 1%, 5%, and 8% by weight of cement. The findings revealed that the incorporation of AC enhanced the mechanical properties of mortar mixtures. Compressive strength increased by up to 20%, while flexural strength improved by roughly 15% relative to normal mortar. At 28 days, the compressive strength of the MP1% mixture attained 53.3 MPa, in contrast to 19.2 MPa at 2 days, indicating there can be significant long-term strength progression. When combining 5% MP with 28 days curing conditions, the pressure was 46.8 MPa. As demonstrated by Scanning Electron Microscopy (SEM), the AC had reacted with the cement matrix and yielded a denser microstructure with fewer voids. FTIR and XRD analysis confirmed the formation of new chemical bonds related to AC's pozzolanic activity that improved the mechanical properties. In this paper, a new method is reported for incorporating Cr-containing activated carbon into cementitious material, offering an eco-friendly method for treating hazardous waste, and is in good accordance with a sustainable economy in transit.

© 2026 MIM Research Group. All rights reserved.

## 1. Introduction

During Durable leather products are inherently reliant on the leather tanning business. Still, it significantly contributes to environmental damage, particularly through wastewater, which includes trivalent chromium (Cr(III)). Despite the fact being less hazardous than hexavalent chromium (Cr(VI)), Trivalent chromium (Cr(III)) poses major ecological and health risks. Chromium salts stabilize collagen fibers in skins during the chrome tanning process, increasing the leather's lifetime. Nearly 90% of tanning companies use basic chrome sulfates [1], which allow only around 60% of chromium to pass through the hides and waste, 40% of which is discharged into

\*Corresponding author: [a.a.amin@univ-adrar.edu.dz](mailto:a.a.amin@univ-adrar.edu.dz)

<sup>a</sup>orcid.org/0009-0007-6140-2096; <sup>b</sup>orcid.org/0000-0002-8547-6811; <sup>c</sup>orcid.org/0009-0002-4908-9037;

<sup>d</sup>orcid.org/0000-0002-8529-7063

DOI: <http://dx.doi.org/10.17515/resm2025-977me0618rs>

Res. Eng. Struct. Mat. Vol. 12 Iss. 3 (2026) 1487-1499

wastewater [2]. Cr(III) has environmental ramifications, including the fact that Cr(III) could leak into surface and groundwater, compromising aquatic ecosystems and sources of drinkable water.

Treatment of tannery effluent can lead to chromium deposits in the soil, compromising the soil quality and plant life. Extended Cr(III) exposure can negatively impact aquatic life and cause respiratory and cutaneous problems in humans. Many therapeutic approaches have been developed to minimize these effects, including pharmacological, physical, and biological. To eliminate Cr(III) from wastewater, adsorption using materials such as activated carbon, biochar, or natural clays is effective [3, 4]. Still, neglected utilized adsorbents could become secondary contaminants [5]. Stabilization/solidification (S/S) is a workable waste management technique that combines contaminated adsorbents with cementitious materials. This method immobilizes damaging components, therefore reducing their leachability and environmental impact. By conserving natural resources and lowering greenhouse gas emissions, using industrial byproducts such as fly ash [6] or slag [7] as partial substitutes for cement in the S/S process help to increase sustainability.

The use of biochar in cementitious materials has been examined to enhance concrete's mechanical characteristics and durability [8]. Biochar can augment compressive strength, diminish shrinkage, and improve water retention in cement composites [9]. Utilizing biochar that adsorbs Cr(III) from tannery waste presents a sustainable approach to recycling industrial leftovers while improving materials efficacy [9]. Khushnood et al. (2016) [10] reported that biochar, generated from biomass pyrolysis, showed promise as a cement component. Incorporating biochar derived from hazelnut and peanut shells enhanced the strength of cement paste by as much as 78%, improving toughness and fracture energy [10, 11]. The incorporation of 0.8% biochar by weight-modified fracture trajectories renders them more convoluted [9, 12, 13]. Substituting 5% of cement with hardwood-derived biochar enhanced the compressive strength of mortar, owing to better water retention and internal curing [14]. Research indicates that biochar is a reinforcing filler, enhancing mechanical performance and decreasing porosity via densification [10, 15]. Incorporating 3% peanut shell biochar enhanced the carbonation rate while diminishing the carbonation depth. It additionally advocated for increased hydration products and an elevated level of hydration [16].

This study explores the use of Cr(III)-contaminated activated carbon in cementitious composites with a view to addressing environmental issues and creating sustainable construction. It reports impacts on mechanical performance, chromium immobilization, and industrial waste disposal. Recycling of contaminated waste is aligned with global approaches to dealing with hazardous wastes and could revolutionize policy towards construction waste and promote greener construction practices.

The research conducted various mechanical and microstructural experimental tests to assess the performance of cement-based materials that include activated carbon contaminated with Cr(III). The mechanical properties of the mortars were examined through compressive strength and flexural strength tests, which were carried out at different curing ages: 2, 7, and 28 days. These tests were performed in accordance with the NF EN 196-1 standard. In particular, the researchers employed Scanning Electron Microscopy (SEM), Energy Dispersive X-ray Spectroscopy (EDS), and Fourier-Transform Infrared (FTIR) spectroscopy to investigate microstructural properties. The techniques promoted the visualization of the hydration products, the recognition of chemical bonds, and the understanding of the activated carbon and the cement matrix interaction. The XRD (X-ray Diffraction) technique was employed to study the samples' crystalline structure; hence, it can show the different phases as well as the effect of the chromium contamination on the microstructure of the material. The results are solid and reliable due to the comprehensive experimental methods, which can even indicate the performance of the modified cementitious materials.

## 2. Materials and Methods

### 2.1. Cement and Sand Used

CEM I CRS cement of class 42.5 was used in the current work. The cement manufactured by the SSC BECHAR cement plant is located in the region of BECHAR, Algeria. It has a Blaine-specific surface area (BSSA) of 3,042 cm<sup>2</sup> /g. The chemical composition of the cement is presented in Table 1. Standard siliceous sand was used as a fine aggregate according to NF P18-541 and EN 196-1 specifications. The sand is made of natural quartz with a particle size distribution controlled between 0.08 mm and 2.00 mm. It meets cleanliness and sphericity standards for cement mortar testing. This ensures consistency and repeatability in evaluating mechanical performance.

Table 1. Chemical composition of the cement used

Component	Percentage By Weight (%)	Component	Percentage By Weight (%)
Na <sub>2</sub> O	0.13%	K <sub>2</sub> O	0.80%
MgO	3.55%	CaO	62.16%
Al <sub>2</sub> O <sub>3</sub>	4.24%	Fe <sub>2</sub> O <sub>3</sub>	5.30%
SiO <sub>3</sub>	19.45%	TiO <sub>2</sub>	0.40%
SO <sub>4</sub>	2.20%	C <sub>3</sub> A	2.274%
Cl	0.014%	C <sub>4</sub> AF	16.132%
C <sub>3</sub> S	69.26%	C <sub>2</sub> S	3.53%

### 2.2. Activated Biochar

Commercial activated carbon from coco-net is used, and characterized by an average adsorption kinetic rate and an average activity rate. As a microporous adsorbent, it ensures efficient removal of trace contaminants. Moreover, it is compatible with international standards (AWWA/EN 12903).

### 2.3. Metal Solutions

Solutions of Cr (III) ions were prepared by diluting a stock solution, which was obtained by dissolving a 0,1887 g quantity of Chromium nitrate Cr<sub>2</sub>(SO<sub>4</sub>)<sub>3</sub> in 1000 ml de-ionized water. Fresh dilutions were made for each study with a concentration of 5 ml/l of chromium III.

### 2.4. Batch Adsorption

Batch adsorption experiments were conducted to evaluate the removal efficiency of Cr (III) using commercial activated carbon. The aim was to simulate typical industrial wastewater conditions. Chromium solutions were prepared by dissolving 0.1887 g of chromium nitrate [Cr<sub>2</sub>(SO<sub>4</sub>)<sub>3</sub>] in 1000 mL of deionized water, then diluted to achieve a working concentration of 5 mL/L. Each experiment took place in a 500 mL Erlenmeyer flask that contained 50 mL of Cr (III) solution. The flasks were placed on a mechanical stirrer and agitated at 200 rpm for 120 minutes.



Fig. 1. Manipulation of batch experiment

The pH of the solution remained close to neutral, around 6.5 to 7.0, with no intentional chemical adjustments. This condition mirrored realistic tannery wastewater. After adsorption, the mixtures were filtered through 0.20  $\mu\text{m}$  membrane filters to remove any leftover carbon particles. The contaminated activated carbon was then dried in an oven at 75°C for 24 hours to eliminate excess moisture, ensuring it was stable before being added to cement mixes. This process assured consistency in preparing Cr(III)-contaminated biochar for later stabilization and solidification studies.

### 2.5. Mix Proportion

Four mixtures of mortar were prepared in this work; the formulations are primarily based on the NF EN196-1 standard. The mixtures contain proportions of 1, 5, and 8% contaminated activated biochar, referred to as MP1%, MP5%, and MP8%, respectively, along with the control sample (without activated biochar) labeled as OM. Both the mortar mixes with biochar had a water-cement (W/C) ratio of 0.50.

Prior to the mechanical testing, the mortars were molded to prepare test samples (three samples for each test) with dimensions of 40 mm  $\times$  40 mm  $\times$  160 mm. The mechanical testing was performed at 2, 7, and 28 days. The materials composing the different mortar formulations are taken at laboratory temperature 20°C  $\pm$  1. The weighing was carried out using a balance with an accuracy of  $\pm$  1g, and a relative humidity of at least 50%. After molding, all specimens were immediately placed in a controlled curing chamber kept at 20  $\pm$  2 °C and relative humidity above 95%, following the EN 196-1 standard. The samples remained under these conditions until mechanical testing occurred at 2, 7, and 28 days. This maintained consistent hydration and provided a reliable assessment of strength development for all mortar mixes. Full details of the mix proportion are shown in Table 2.

Table 2. Mix proportion

Designation	Cement (g)	Sand (g)	Water (g)	Activated Biochar (g)	Rapport Water/Cement
MP0%	450	1350	225	0	
MP1%	445.5	1350	225	4.5	0.5
MP5%	427.5	1350	225	22.5	
MP8%	414	1350	225	36	

### 2.7. FTIR, SEM and EDS

Samples from crushed cement pastes were used for the FTIR and SEM analyses. The pastes were ground to a particle size of less than 75  $\mu\text{m}$  and 105  $\mu\text{m}$  (exclusively for the FTIR test) utilizing a manual mortar and pestle. The FTIR analysis technique employed infrared light to examine the test samples and assess their chemical qualities. FTIR Spectroscopy, an analytical method utilized to identify organic, polymeric, and occasionally inorganic substances, was used. SEM pictures examined the microstructure of the cement pastes with biochar, and the semi-quantitative elemental composition was assessed using the EDS connected to the microscope. Samples were analyzed by the Hitachi S-3000N semi-environmental scanning electron microscope with backscattered electrons (BSE) at 20 kV.

### 2.8. Mechanical Strength

Compressive and Flexural strengths were measured on a press-of-type universal testing machine (Zhejiang Lu) with a capacity of 300 KN, piloted by a computer. For each mixture, three specimens (40 mm  $\times$  40 mm  $\times$  160 mm) were tested at 2, 7, and 28 days, according to the NF EN 196-1 standard. The flexural strength test was conducted at a loading rate of 50  $\pm$  10 N/s, and the resulting halves were subsequently used for compressive strength testing at a loading rate of 2400  $\pm$  200 N/s, as prescribed by the standard.

## 2.9.X-Ray Diffraction (XRD) Analysis

XRD examinations were performed to determine the microstructure of crushed mortars. A small amount of powder samples is scanned using an X-ray diffractometer with an angle of  $2\theta$ . X-rays are dispersed by atoms in a model that indicates the mesh spacing of the elements present in the analyzed material. Once the X-ray analysis is completed, the spectra are recorded and analyzed for the specimens using the XPERT-PROF PANALYTICAL diffractometer.

## 3. Results and Discussion

### 3.1 FTIR Analysis

Figure 2 shows the FTIR spectrum for the mixtures MP5%, MP8% and ordinary mortar MPO%. In the MPO% sample, peaks were observed at  $406.90\text{ cm}^{-1}$  (O-H bending) indicating hydration products such as calcium hydroxide.  $620.96\text{ cm}^{-1}$ ,  $709.66\text{ cm}^{-1}$ ,  $831.16\text{ cm}^{-1}$ , and  $894.79\text{ cm}^{-1}$  (C-H out-of-plane bending), indicating the presence of various organic compounds and possibly unreacted components of the mortar mix. These peaks exhibit complex functional groups, including carbonyl compounds, nitriles, thiols, alkanes, and amines. This indicates the presence of specific chemical structures not found in MP5% and MP8%.

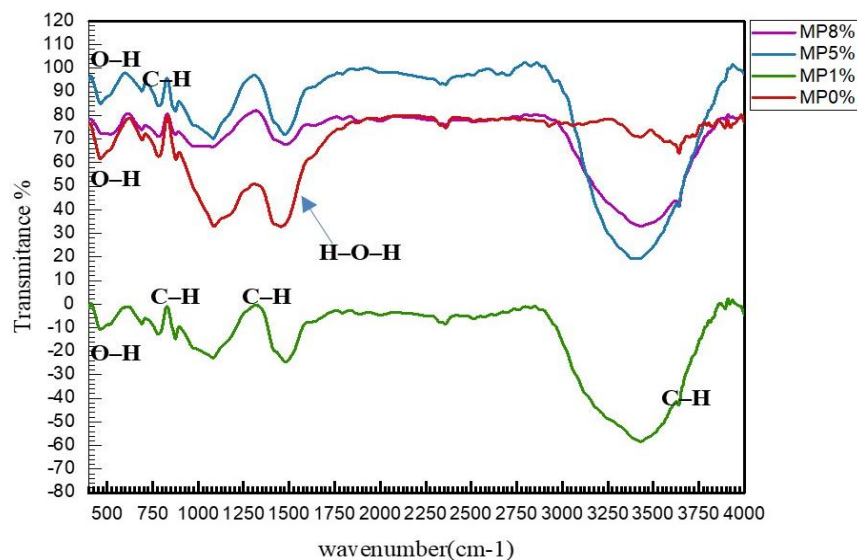


Fig. 2. FTIR spectrum for the Different mixtures of mortar

For MP8%, the FTIR spectrum displayed key peaks at  $831.16\text{ cm}^{-1}$ ,  $1303.62\text{ cm}^{-1}$ , and  $3910.87\text{ cm}^{-1}$ , corresponding to C-H out-of-plane bending, C-O stretching, and O-H stretching, respectively. These peaks indicate the presence of alcohols, esters, ethers, and phenols. MP5% showed similar peaks at the same wavenumbers but with higher intensities, suggesting a greater concentration of these functional groups than MP8%.

### 3.2 Mechanical Strength

Mechanical tests, including compressive and flexural tests, were carried out at the ages of 2 days, 7 days and 28 days using Zhejiang Lu da Mechanical Instruments LTD 300 kN. Figure 3 shows the compressive strength of mortar mixes at 2, 7, and 28 days of age; from 2 days to 28 days, all samples displayed a similar increasing trend. Strong strength development at 28 days was evident in the MP1% sample as the compressive strength rose steadily from 19.2 MPa at two days to 53.3 MPa at 28 days. Conversely, MP5% attained the highest strength after 2 days; however, its strength at 28 days was lower than that of MP1%, suggesting a faster initial setting associated with slower strength development at 28 days. While MP5% attained a similar 28 days strength of 46.8 MPa at 28 days, MP1% regularly shows lower strengths. At all levels, MP8% displayed the lowest strength among the MP samples. Though there is no direct link, Sirico et al. (2020) [17] claimed that the high C-S-H concentration of biochar correlates with the rise in compressive strength.

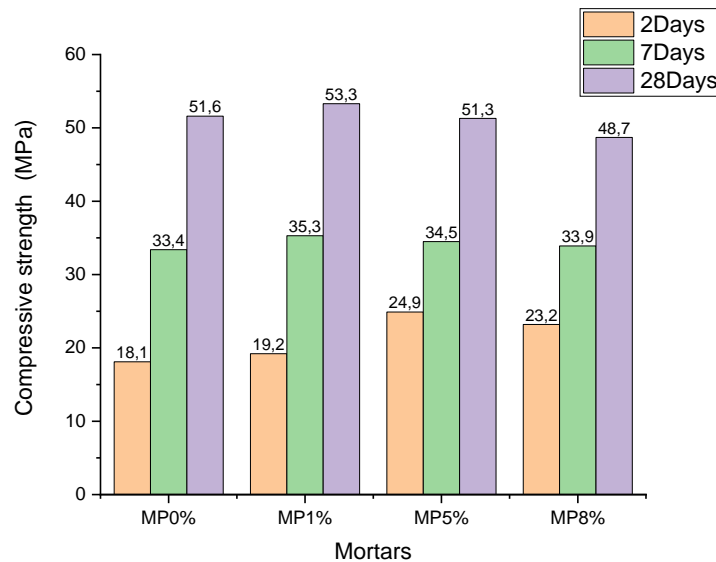


Fig. 3. Compressive strength of mortars mixes at 2days,7 days and 28day ages

The observed increase in compressive strength, especially at 1% biochar content, can be attributed to the water-retention ability of activated carbon and its potential to improve internal curing, as Gupta et al. (2018) [9] noted. The water retained during mixing and storing samples can evaporate, leaving behind large capillary holes, which diminishes compressive strength; activated Biochar could absorb that water, increasing its strength [18].

In a prior study, it was demonstrated that the inclusion of a lower percentage of biochar increases compressive strength because it facilitates cement hydration, whereas the use of a high percentage of biochar as an additive diminishes strength due to biochar's porosity and brittleness [19]. Several studies on biochar indicate that the addition of a smaller amount of biochar increases compressive strength [20], and [18]. Nonetheless, certain researchers say a high optimal proportion of biochar addition can boost compressive strength [21, 22]. This finding aligns with the internal curing process described in high-performance concretes. Additionally, contaminated biochar can increase strength without affecting hydration chemistry, suggesting that it serves two purposes: improving structure and aiding environmental clean-up efforts. This initiative supports the global development of sustainable building materials and strategies for the reuse of hazardous waste.

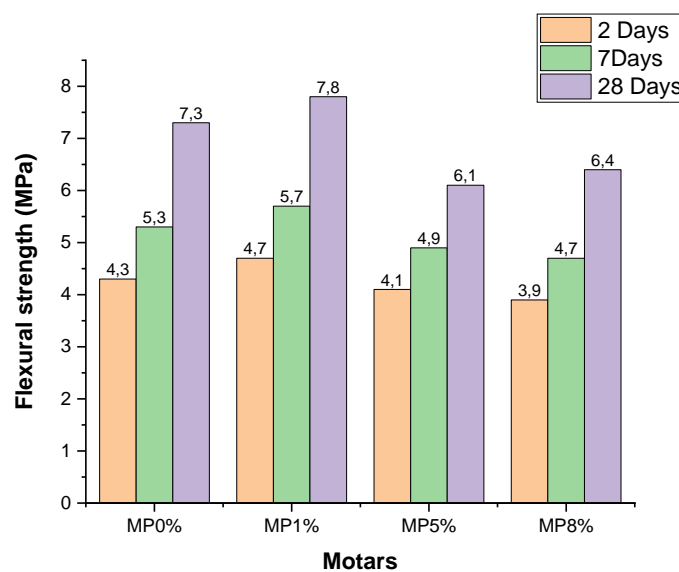


Fig. 4. Flexural strength of concrete mixes at 2days,7days and 28day ages

The increase in strength attributed to the incorporation of activated carbon was associated with its water absorption and retention ability [9]. In the concrete mixing process, dry activated carbon

particles absorbed a portion of the mixing water, leading to a reduced free water-cement ratio in the concrete matrix. The elevated presence of capillary water results in increased capillary porosity within the cementitious matrix [23], adversely affecting strength development [24]. The absorption of water by porous activated biochar resulted in the densification of the cement matrix by decreasing the free water within the pores of concrete during the early hardening phase. The water absorbed in the pores of activated biochar was subsequently utilized internally to provide hydration support for cement through internal curing, hence enhancing the strength of the cementitious matrix.

The reductions in flexural strength of cement mortar at 7 days and 28 days, resulting from the substitution of cement with activated biochar, are illustrated in Figure 4. An ideal cement percentage of 1% by weight can be calculated to yield a modest enhancement in the flexural strength of mortar akin to ready-mix concrete [25]. The presence of air spaces created by the incorporation of activated biochar particles diminishes the influence of adding either dry or pre-soaked biochar on the development of flexural strength.

### **3.3. XRD Results**

XRD patterns show striking changes in both the crystal quality and structure of the cement reactivated carbon, due to the trivalent chromium, by Xylenes AND water (SPOTA). A peak of the activated carbon and silicate aggregates in the mortar was observed at  $26.5^\circ$  of  $2\theta$ . No secondary peaks of calcium silicate hydrates, portlandite, and silicate minerals were found in the angular region between  $20^\circ \sim 68^\circ$  of  $2\theta$ . Lack of a peak associated with trivalent chromium compounds probably demonstrates incorporation in an amorphous state or ultra-low concentration. Carbon-cement formation, based on the peak intensification of the main peak as a structure-interaction favorable tendency.

### **3.4. SEM / EDS Results**

The scanning electron microscopy [26] pictures in Figure 6 (a, b, c, and d) illustrate the formation of hydration products within the pores of the activated biochar. 1% Chromium on SEM image (100%) shows embryonic crystalline development on a so-far fairly smooth surface. Most probably produced in low chromium amounts [27, 28] from formed Cr-hydrates with Cr, or Cr-ettringite, these young crystals are harmless to the cement matrix, so the inclusion of chromium in hydration products hardly affects the cohesivity when present at such a low concentration. Standard products like C-S-H and ettringite are still being formed; the hydration of cement is barely modified; the strength and somewhat acceptable mechanical integrity stay in place [29], [30].

As the level of chromium is increased to 5%, larger crystalline structures and higher surface roughness are characterized by a defined surface morphology. In this alteration, it is suggested that the more important interests of chromium during this hydration process are most likely participating in the generation of chromium-induced compounds [phases based on Ca-Cr oxides or Cr sulphate [31]]. These ingredients may provide a barrier to the migration of hydration products around cement particles, thereby permanently slowing the hydration rate and maybe the early compressive strength of the mortar; SEM images from the surface show a rather dirty-looking morphology (Figure 6), indicating a rougher surface and indicative of a potential extension of setting time for cement material likely to impact the initial strength of the material [32].

The SEM image displays notable crystalline development at 8% chromium with uneven-perfect surface morphology. This crystallization suggests a higher concentration of Cr, probably forming large-sized Cr-ettringite crystals with these big crystalline structures. The huge crystalline structures here dissolve the cement matrix and may conceivably obviate phases due to chromium for something in the matrix. The occurrence can be considered a "dilution effect" on the hydration process that compromises the structural durability of the material, and in doing so yields a reduction in its compressive strength [8]. This SEM image highlights the extensive disorder introduced by high levels of Cr and hence, provides a verification that beyond a certain threshold, the mechanical properties of the material will be compromised. [8]. SEM Image, Source defects and fractures illustrated have a great impact on the addition of high chromium, as it becomes clear from

the surface [33]; therefore, validating that excessive chromium content could lead to deterioration of the mechanical properties of the material.

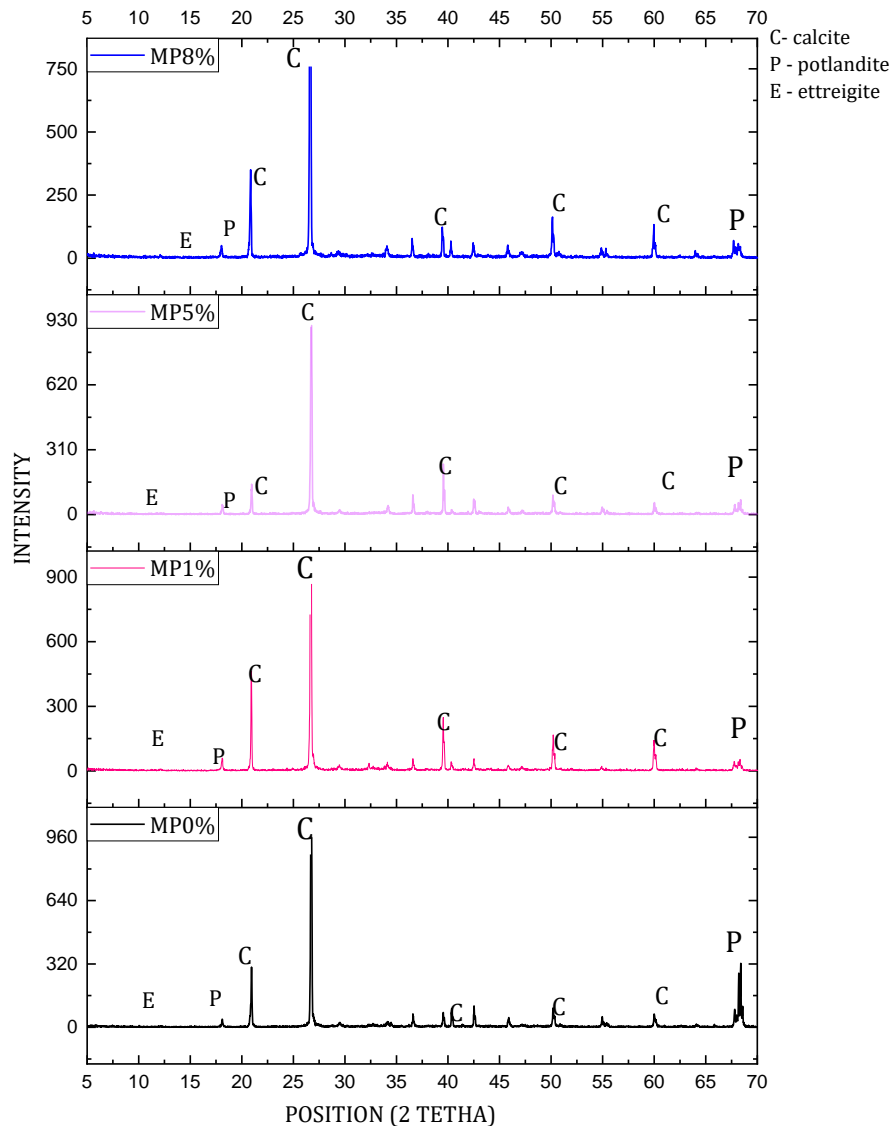
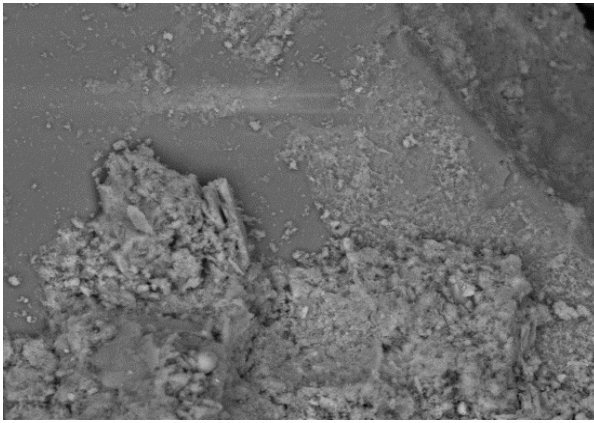


Fig. 5. XRD spectrum of different Mortars

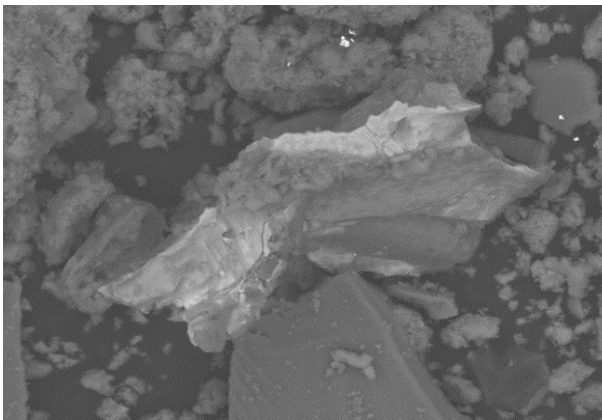
Alternatively, the activated biochar pores absorb water during mortar mixing, creating a wet environment that promotes the development of calcium silicate hydrate C-S-H gel, calcium hydroxide, and ettringite. Furthermore, localized carbonation induced by the biochar results in the creation of calcium carbonate crystals. C-S-H is an essential binder in cementitious mortar, and its strength contribution is evident when it integrates into the mortar matrix, adhering the biochar particle to the mortar paste. Consequently, the accumulation of C-S-H and calcium hydroxide within these pores is not expected to enhance strength growth. [34]

The analysis of EDS spectra from four samples of mortar doped with different chromium contents reveals significant modifications in the elemental composition, directly related to the evolution of the chemical and microstructural behavior of the cement matrix. The control sample, free of chromium, shows a typical composition of hydrated cement, with a predominance of oxygen 57.42%, silicon 23.99%, and calcium 11.81%, confirming the major presence of C-S-H phases (calcium silicate hydrate) and ettringite. This configuration is typical of classic Portland cements, where the hydration products ensure the cohesion and strength of the matrix [35, 36].



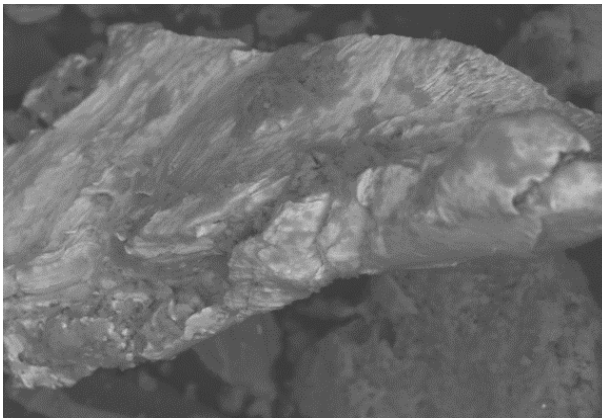
Elément	A	Net	Mass. norm. [%]	Atom. [%]	erreur abs. [%] (1 sigma)	erreur rel. [%] (1 sigma)
O	8	5163	57,42	73,06	2,62	4,25
Si	14	5006	23,99	17,39	1,92	7,47
Ca	20	1633	18,11	9,20	1,91	9,86
Al	13	133	0,47	0,36	0,09	18,79
		<b>Total:</b>	<b>100,00</b>	<b>100,00</b>		

(a)



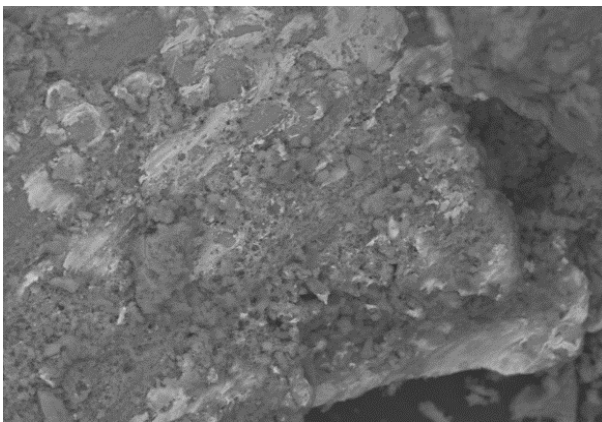
Elément	A	Net	Mass. norm. [%]	Atom. [%]	erreur abs. [%] (1 sigma)	erreur rel. [%] (1 sigma)
O	8	1720	22,32	44,23	1,28	5,16
Al	13	173	1,17	1,37	0,20	15,12
Si	14	1374	11,23	12,67	1,07	8,58
Ca	20	1334	18,05	14,28	1,91	9,55
Cr	24	242	8,51	5,19	1,42	15,07
Fe	26	445	38,10	21,63	6,68	15,82
S	16	87	0,64	0,63	0,15	21,28
		<b>Total:</b>	<b>100,00</b>	<b>100,00</b>		

(b)



Elément	A	Net	Mass. norm. [%]	Atom. [%]	erreur abs. [%] (1 sigma)	erreur rel. [%] (1 sigma)
O	8	3103	19,82	42,58	0,82	4,54
Si	14	1274	5,67	6,94	0,37	7,20
Ca	20	1616	12,02	10,31	0,78	7,15
Cr	24	569	11,89	7,86	1,15	10,63
Fe	26	982	48,81	30,04	5,09	11,42
Al	13	292	1,07	1,36	0,13	13,15
Mg	12	99	0,40	0,57	0,10	28,15
S	16	79	0,31	0,34	0,09	29,95
		<b>Total:</b>	<b>100,00</b>	<b>100,00</b>		

(c)



Elément	A	Net	Mass. norm. [%]	Atom. [%]	erreur abs. [%] (1 sigma)	erreur rel. [%] (1 sigma)
O	8	3513	25,46	47,63	1,15	4,70
Mg	12	237	0,75	0,92	0,11	15,43
Si	14	3077	10,90	11,62	0,65	6,25
Ca	20	3851	24,86	18,57	1,57	6,60
Fe	26	722	30,43	16,31	3,38	11,61
Cr	24	320	6,51	3,75	0,76	12,24
Al	13	378	1,09	1,21	0,12	11,49
		<b>Total:</b>	<b>100,00</b>	<b>100,00</b>		

(d)

Fig. 6. SEM / EDS analysis of different mortars: a(MP0%),b(MP1%),c(MP5%), and d(MP8%)

When the chromium content reaches about 5%, significant alterations are observed. Chrome rises to 5.19%, while iron becomes the majority component 38.10%, leading to a relative decrease in calcium, silica, and oxygen. This redistribution indicates that chromium does not merely act as a passive element but actively interacts with the hydrated phases, particularly by forming compounds such as Cr-ettringite, identified under conditions of aluminum substitution by chromium in Aft structures [3, 32, 37]. These phases can slow down hydration reactions by forming passivating layers around clinker grains [38], which explains a possible decrease in mechanical performance observed in previous studies on chromium-doped cements [39].

When the chromium concentration reaches 7.86%, the disruptive effect becomes evident. Iron reaches nearly 49%, chromium 7.86%, while silica drops to 5.67%. This evolution indicates a saturation of the matrix by secondary metallic phases. The excessive formation of chrome ferrites or mixed Cr-Fe oxides strongly disrupts the formation of structuring hydrates, leading to a decrease in the density of the cement matrix, which has been correlated with a loss of mechanical strength in several studies [39, 40]. This phenomenon is often referred to as the dilution effect, where the cementitious constituents are partially replaced by non-hydrating compounds.

However, the sample containing 6.51% chromium seems to represent a form of compromise. Despite a high iron concentration 30.44%, the proportions of oxygen 25.46%, calcium 13.63%, and silicon 10.90% remain relatively balanced. This configuration suggests a better integration of chromium into the matrix, through stabilized phases that do not completely inhibit hydration. Such observations confirm the results of Zhang et al. (2021) [31], who showed that a moderate concentration of chromium allows for the effective immobilization of this metal while maintaining a sufficiently coherent cement structure. This dual function—mechanical and environmental—reinforces the viability of using cement as a stabilization matrix for industrial waste containing heavy metals, provided that critical concentration thresholds are respected.

In summary, the present analysis highlights a direct correlation between chromium concentration and the gradual modification of the cement microstructure. If low concentrations allow for relatively neutral incorporation, high levels cause significant disorganization of the matrix, compromising both the hydration kinetics and mechanical performance. The optimization of chromium content thus represents a major challenge for waste stabilization applications, at the interface between technical performance and environmental sustainability.

#### **4. Conclusions**

This study investigates the incorporation of activated carbon contaminated with trivalent chromium (Cr(III)) into cementitious materials, emphasizing its effects on mechanical properties, microstructure, and chromium stabilization. The results from compressive and flexural strength tests, as well as FTIR, SEM/EDS, and XRD analyses, offer beneficial information about the interactions between Cr(III) and the cement matrix, as well as the overall performance of the modified cementitious materials; and the following conclusions are drawn:

- The presence of Cr(III) in contaminated activated carbon affects the behavior of cementitious materials, particularly regarding hydration and microstructure. With 1% biochar addition, the chromium level remained low and did not significantly interfere with the hydration process. EDS and XRD analyses showed that Cr(III) interacted with hydration products of cement, leading to the formation of stable compounds such as Cr-ettringite, which help immobilize chromium and mitigate its environmental effects. However, at higher biochar levels (5% and 8%), the interaction between chromium and the cement phases intensified, resulting in decreased hydration efficiency and the creation of less stable microstructures, a phenomenon attributed to the dilution effect that chromium compounds have on typical hydration product development.
- Mechanical testing indicated that the addition of biochar greatly enhanced compressive and flexural strength, especially at 1% biochar, where compressive strength improved by approximately 20%. In contrast, higher biochar levels (5% and 8%) resulted in lower strength, likely due to chromium interfering with hydration and increased porosity caused by the biochar.

- FTIR analysis verified the creation of new pozzolanic bonds, suggesting that biochar plays an active role in cement hydration. Supporting evidence from SEM/EDS and XRD results showed enhanced microstructure at low biochar concentrations, whereas higher amounts disrupted crystallinity and hydration, adversely affecting long-term performance.
- Activated biochar at levels of 1%, 5%, and 8% was primarily selected to enable items to retain their mechanical properties as well as to prevent their possible negative impacts. It was initially assumed that the 1% concentration of activated biochar would not only fortify the material but also have a minimal disruptive effect on the cement matrix. Nevertheless, higher concentrations were examined to understand their influence on hydration and the overall material performance. In field usage, there are some problems, for example, the long-term use of the product, which causes durability issues, variations in biochar properties, and the possibility of secondary contamination because of the incorrectly processed biochar. Nevertheless, 5% and 8% activated biochar had higher porosity and uneven distribution that resulted in lower compressive strength.

In summary, using activated biochar in cement materials shows great promise. It can improve the mechanical properties of construction materials and help mitigate environmental problems caused by heavy metal pollution. This technology allows for sustainable waste use and supports green chemistry and the circular economy by incorporating trivalent chromium (Cr (III)) in a stable cement mix. However, we need to acknowledge some limitations. We need to assess the long-term durability of the composite materials and how their breakdown products behave in the environment. Differences in the chemical makeup and physical traits of Cr (III)-contaminated activated biochar may influence the consistency and reliability of the results. Additionally, findings from controlled lab settings may not fully capture the complexities of real-world scenarios, making it harder to apply the results broadly. Future research should focus on testing the long-term effectiveness and environmental safety of these composites in various weather and operating conditions to confirm their practical use in sustainable construction and waste management.

## Acknowledgement

The authors acknowledge that this study is supported by ADRAR University and the Laboratory of Sustainable Development and IT, LDDI.

## References

- [1] Aravindhan R, Madhan B, Rao JR, Nair BU, Ramasami T. Bioaccumulation of Chromium from Tannery Wastewater: An Approach for Chrome Recovery and Reuse. *Environmental Science & Technology*. 2004;38(1):300-6. <https://doi.org/10.1021/es034427s>
- [2] Fabiani C, Ruscio F, Spadoni M, Pizzichini M. Chromium(III) salts recovery process from tannery wastewaters. *Desalination*. 1997;108(1):183-91. [https://doi.org/10.1016/S0011-9164\(97\)00026-X](https://doi.org/10.1016/S0011-9164(97)00026-X)
- [3] Feng Y, Yang S, Xia L, Wang Z, Suo N, Chen H, et al. In-situ ion exchange electrocatalysis biological coupling (i-IEEBC) for simultaneously enhanced degradation of organic pollutants and heavy metals in electroplating wastewater. *Journal of Hazardous Materials*. 2019;364:562-70. <https://doi.org/10.1016/j.jhazmat.2018.10.068>
- [4] Krausmann F, Erb KH, Gingrich S, Lauk C, Haberl H. Global patterns of socioeconomic biomass flows in the year 2000: A comprehensive assessment of supply, consumption and constraints. *Ecol Econ*. 2008;65(3):471. <https://doi.org/10.1016/j.ecolecon.2007.07.012>
- [5] Ali I, Asim M, Khan TA. Low cost adsorbents for the removal of organic pollutants from wastewater. *Journal of environmental management*. 2012;113:170-83. <https://doi.org/10.1016/j.jenvman.2012.08.028>
- [6] Ganesh AC, Kumar MV, Mukilan K, Kumar AS, Kumar KA. Investigation on the effect of ultra fine rice husk flashover slag based geopolymer concrete. *Research on Engineering Structures & Materials*. 2023;9(1):67-81. <http://dx.doi.org/10.17515/resm2022.501ma0814>
- [7] Noui Ar, Belkadi AA, Zeghichi L, Kessal O, Bouglada MS, Achour Y, Gomes JC. Improving early strength and durability of eco-friendly mortars: Investigating the influence of limestone filler fineness and blast furnace slag combination. *Res. Eng. Struct. Mater.*, 2025; 11(2): 443-463. <http://dx.doi.org/10.17515/resm2024.226ma0407rs>
- [8] Liu J, Wu D, Tan X, Yu P, Xu L. Review of the Interactions between Conventional Cementitious Materials and Heavy Metal Ions in Stabilization/Solidification Processing. *Materials*. 2023;16(9):3444. <https://doi.org/10.3390/ma16093444>

- [9] Gupta S, Kua HW, Koh HJ. Application of biochar from food and wood waste as green admixture for cement mortar. *Science of The Total Environment*. 2018;619-620:419-35. <https://doi.org/10.1016/j.scitotenv.2017.11.044>
- [10] Khushnood RA, Ahmad S, Restuccia L, Spoto C, Jagdale P, Tulliani J-M, et al. Carbonized nano/microparticles for enhanced mechanical properties and electromagnetic interference shielding of cementitious materials. *Frontiers of Structural and Civil Engineering*. 2016;10(2):209-13. <https://doi.org/10.1007/s11709-016-0330-5>
- [11] Restuccia L, Reggio A, Ferro GA, Kamranirad R. Fractal analysis of crack paths into innovative carbon-based cementitious composites. *Theoretical and Applied Fracture Mechanics*. 2017;90:133-41. <https://doi.org/10.1016/j.tafmec.2017.03.016>
- [12] Haselbach L, Thomas A. Carbon sequestration in concrete sidewalk samples. *Construction and Building Materials*. 2014;54:47-52. <https://doi.org/10.1016/j.conbuildmat.2013.12.055>
- [13] Bertos MF, Simons S, Hills C, Carey P. A review of accelerated carbonation technology in the treatment of cement-based materials and sequestration of CO<sub>2</sub>. *Journal of hazardous materials*. 2004; 112(3):193-205. <https://doi.org/10.1016/j.jhazmat.2004.04.019>
- [14] Roberts KG, Gloy BA, Joseph S, Scott NR, Lehmann J. Life Cycle Assessment of Biochar Systems: Estimating the Energetic, Economic, and Climate Change Potential. *Environmental Science & Technology*. 2010;44(2):827-33. <https://doi.org/10.1021/es902266r>
- [15] Ahmad S, Khushnood RA, Jagdale P, Tulliani J-M, Ferro GA. High performance self-consolidating cementitious composites by using micro carbonized bamboo particles. *Materials & Design*. 2015; 76:223-9. <https://doi.org/10.1016/j.matdes.2015.03.048>
- [16] Gupta S, Muthukrishnan S, Kua HW. Comparing influence of inert biochar and silica rich biochar on cement mortar - Hydration kinetics and durability under chloride and sulfate environment. *Construction and Building Materials*. 2021;268:121142. <https://doi.org/10.1016/j.conbuildmat.2020.121142>
- [17] Sirico A, Bernardi P, Belletti B, Malcevschi A, Dalcanale E, Domenichelli I, et al. Mechanical characterization of cement-based materials containing biochar from gasification. *Construction and Building Materials*. 2020;246:118490. <https://doi.org/10.1016/j.conbuildmat.2020.118490>
- [18] Porter, D. *Renewable Energy Policy and Incentives*. Wiley-Blackwell, 2012: ISBN 978-1-118-26872-4. <https://doi.org/10.1016/B978-0-08-087872-0.00901-X>
- [19] Lee, J.W. *Advanced Biofuels and Bioproducts*. Springer Science & Business Media, 2012: ISBN 978-1-4614-6434-1, DOI: 10.1007/978-1-4614-6435-8. <https://doi.org/10.1007/978-1-4614-6435-8>
- [20] Wang, S., & Luo, Z. *GREEN Alternative Energy Resources*. CRC Press, 2017: ISBN 978-1-4987-2832-3.
- [21] Camacho Y, Bensaid S, Ruggeri B, Restuccia L, Ferro G, Mancini G, et al. Valorisation of by-products/waste of agro-food industry by the pyrolysis process. *Journal of Advanced Catalysis Science and Technology*. 2016;3:1-11. <https://doi.org/10.15379/2408-9834.2016.03.01.01>
- [22] Lam C, Barford JP, McKay G. Utilization of incineration waste ash residues in Portland cement clinker. *Chemical Engineering*. 2010;21:757-62.
- [23] Espinoza-Hijazin G, Lopez M. Extending internal curing to concrete mixtures with W/C higher than 0.42. *Construction and Building Materials*. 2011;25(3):1236-42. <https://doi.org/10.1016/j.conbuildmat.2010.09.031>
- [24] Aïtcin P-C, Mindess S. *Sustainability of concrete*: Crc Press; 2011. <https://doi.org/10.1201/9781482266696>
- [25] Zhao S-X, Ta N, Wang X-D. Effect of temperature on the structural and physicochemical properties of biochar with apple tree branches as feedstock material. *Energies*. 2017;10(9):1293. <https://doi.org/10.3390/en10091293>
- [26] Damidot D, Nonat A, Barret P, Bertrandie D, Zanni H, Rassem R. C3S hydration in diluted and stirred suspensions:(III) NMR study of CSH precipitated during the two kinetic steps. *Advances in cement research*. 1995;7(25):1-8. <https://doi.org/10.1680/adcr.1995.7.25.1>
- [27] Deng Q, Lai Z, Yan T, Wu J, Liu M, Lu Z, et al. Effect of Cr (III) on hydration, microstructure of magnesium phosphate cement, and leaching toxicity evaluation. *Environmental Science and Pollution Research*. 2021;28(12):15290-304. <https://doi.org/10.1007/s11356-020-11780-2>
- [28] Pang F, Wei C, Zhang Z, Wang W, Wang Z. The migration and immobilization for heavy metal chromium ions in the hydration products of calcium sulfoaluminate cement and their leaching behavior. *Journal of Cleaner Production*. 2022;365:132778. <https://doi.org/10.1016/j.jclepro.2022.132778>
- [29] Sinyoung S, Songsiriritthigul P, Asavapisit S, Kajitvichyanukul P. Chromium behavior during cement-production processes: a clinkerization, hydration, and leaching study. *Journal of hazardous materials*. 2011;191(1-3):296-305. <https://doi.org/10.1016/j.jhazmat.2011.04.077>
- [30] OPROIU C-L, PARVAN G, VOICU G, BADANIOIU A-I, TRUSCA R. Influence of a Chromium-rich Industrial Waste on the Hydration and Hardening Processes of Portland Cements with Slag and Limestone Additions.

- [31] Zhao R, Zhang L, Guo B, Chen Y, Fan G, Jin Z, et al. Unveiling substitution preference of chromium ions in sulphoaluminate cement clinker phases. *Composites Part B: Engineering*. 2021;222:109092. <https://doi.org/10.1016/j.compositesb.2021.109092>
- [32] Wang J, Chen F, Yu R, Fan D, Zhang T. Effect of heavy metal (Mn, Pb and Cr) on the properties and hydration in low water/binder cement-based composites (LW/B-CC). *Construction and Building Materials*. 2023;386:131567. <https://doi.org/10.1016/j.conbuildmat.2023.131567>
- [33] Belebchouche C, Bensebti S-E, Ould-Said C, Moussaceb K, Czarnecki S, Sadowski L. Stabilization of Chromium Waste by Solidification into Cement Composites. *Materials*. 2023;16(18):6295. <https://doi.org/10.3390/ma16186295>
- [34] Amina A, Lyacine B, Benamar B, Nassim K. Experimental investigation of the incorporation of trivalent chromium-contaminated activated carbon into cementitious materials. *Studies in Engineering and Exact Sciences*. 2024;5(2):e6476-e. <https://doi.org/10.54021/seesv5n2-081>
- [35] Taylor, H.F.W. *Cement Chemistry*, 2nd ed., Thomas Telford, London, 1997: ISBN 978-0-7277-3945-2.
- [36] Hewlett P, Liska M. *Lea's chemistry of cement and concrete*: Butterworth-Heinemann; 2019. <https://doi.org/10.1016/B978-0-08-100773-0.00014-9>
- [37] Guo J, Luo C. Risk assessment of hazardous materials transportation: A review of research progress in the last thirty years. *Journal of traffic and transportation engineering (English edition)*. 2022;9(4):571-90. <https://doi.org/10.1016/j.jtte.2022.01.004>
- [38] Antico F, De la Varga I, Esmaeli H, Nantung T, Zavattieri P, Weiss W. Using accelerated pavement testing to examine traffic opening criteria for concrete pavements. *Construction and Building Materials*. 2015;96:86-95. <https://doi.org/10.1016/j.conbuildmat.2015.07.177>
- [39] Lothenbach B, Scrivener K, Hooton R. Supplementary cementitious materials. *Cement and concrete research*. 2011;41(12):1244-56. <https://doi.org/10.1016/j.cemconres.2010.12.001>
- [40] Berra M, Carassiti F, Mangialardi T, Paolini AE, Sebastiani M. Effects of nanosilica addition on workability and compressive strength of Portland cement pastes. *Construction and Building Materials*. 2012;35:666-75. <https://doi.org/10.1016/j.conbuildmat.2012.04.132>